Article

Influence of Pt Ultrathin Interlayers on Magnetic Anisotropy in Ni/NiO Multilayers

Dimitrios I. Anyfantis [1,*] **, Alexandros Barnasas** [1,†] **, Nikolaos C. Diamantopoulos** [1] **, Constantinos M. Tsakiris** [1] **, Georg Schmidt** [2,3] **, Evangelos Th. Papaioannou** [2,4] **and Panagiotis Poulopoulos** [1]

[1] Department of Materials Science, School of Natural Sciences, University of Patras, 26504 Patras, Greece; mparnalex@gmail.com (A.B.); msci1300@ac.upatras.gr (N.C.D.); msci885@upnet.gr (C.M.T.); poulop@upatras.gr (P.P.)

[2] Institut für Physik, Martin-Luther University Halle-Wittenberg, Von-Danckelmann-Platz 3, 06120 Halle, Germany; georg.schmidt@physik.uni-halle.de (G.S.); epapaioa@auth.gr (E.T.P.)

[3] Interdisziplinäres Zentrum für Materialwissenschaften, Nanotechnikum Weinberg, Martin-Luther University Halle-Wittenberg, Heinrich-Damerow-Str. 4, 06120 Halle, Germany

[4] Department of Physics, Aristotle University of Thessaloniki, 54124 Thessaloniki, Greece

* Correspondence: up1057157@upatras.gr

† Current address: Department of Physics and Astronomy, Uppsala University, P.O. Box 516, SE-75120 Uppsala, Sweden.

Abstract: Perpendicular magnetic anisotropy at transition metal/oxide interfaces plays a significant role in technological applications such as magnetic storage and spintronics. In this study, we investigate the effects of thermal annealing and Pt ultrathin interlayers on the magnetic anisotropy in Ni/NiO multilayers. Ni/NiO/Pt multilayers were fabricated via radiofrequency magnetron sputtering and natural oxidation. The static magnetic properties of the samples were studied using temperature-dependent SQUID magnetometry. We focus on a sample with a Nickel thickness of 6.7 nm in each multilayer period. This multilayer in Ni/NiO form showed the maximum enhancement of perpendicular magnetic anisotropy after mild thermal annealing in past work. In this work, we study the effects of ultrathin Pt interlayers on the magnetic properties of such a Ni/NiO multilayer before and after annealing. We have observed a further increase in perpendicular magnetic anisotropy, and we study the temperature-dependent magnetic properties of this system, which combines the favorable magnetic properties of Ni/Pt and Ni/NiO multilayers.

Keywords: magnetic multilayers; magnetic anisotropy; growth; sputtering; transition metal oxides; Ni; NiO; Pt

1. Introduction

The discovery of perpendicular magnetic anisotropy (PMA) in Co/Pd multilayers at IBM laboratories [1] and significant magneto-optical Kerr rotation in similar systems [2] brought multilayer films to the center of research interest for the construction of high-density magnetic and magneto-optical recording media [3,4]. In a brief letter, Krishnan et al. first reported the presence of perpendicular anisotropy in the Ni/Pt system developed with e-beam evaporation [5]. Later, in 1997, Angelakeris et al. [6] and Shin et al. [7] published articles on this system using films fabricated by e-beam evaporation and dc magnetron sputtering, respectively. The first one described the magnetic and magneto-optical properties of the system, while Shin focused only on magnetic properties.

The existence of enhanced magnetization due to spin-polarized platinum on the Ni/Pt interface was later confirmed through X-ray magnetic circular dichroism experiments (XMCD) [8]. Thus, the reported reduced magnetization in [7,9] seemed to be due to some interdiffusion of nickel and platinum at the interface, as in the sputtering process, the atoms have much larger kinetic energies than in e-beam evaporation [10]. An interesting

observation in both works was that not only for thin nickel layers but also for very thin platinum layers (platinum thickness t_{Pt} at about 0.3–0.4 nm) and relatively thicker nickel layers (nickel thickness t_{Ni} at about 1.5 nm), Ni/Pt multilayers exhibited perpendicular magnetic anisotropy [6,7]. Additionally, both works suggested that magnetoelastic anisotropy due to strain is responsible for the appearance of perpendicular magnetic anisotropy in Ni/Pt multilayers. Furthermore, Krishnan et al., in a previous work, showed that there is also a contribution of surface anisotropy, K_S, that was found for the first time to have a positive sign (favoring PMA) in a Ni/Pt multilayer system deposited at 473 K and measured at 5 K [11].

On the one hand, magnetic multilayers with thin layers of metal oxides have gained attention owing to the emergence of tunneling magnetoresistance phenomena [12,13]. Subsequently, these multilayers have been investigated for applications in recording media and spintronics [14–16]. Of particular interest are multilayers featuring thin layers of oxides derived from magnetic metals such as Ni and Co, as they have the capability to induce the exchange bias phenomenon in both multilayers and films [17]. The latter can be strategically applied in antiferromagnetic spintronics [18].

Thin nickel oxide layers, NiO, with a thickness of about 1 nm, can be obtained by oxidizing metallic Ni under vacuum conditions and introducing either oxygen or air into the chamber [19,20]. Experimental and theoretical works suggest that for metal/oxide interfaces, PMA could be the result of electronic hybridization between the oxygen and the magnetic transition metal orbits across the interface [21–23]. Additionally, Ni/NiO multilayer films were developed with a tendency for perpendicular anisotropy and a K_S value of +0.11 erg/cm^2 at room temperature and +0.135 erg/cm^2 at 5 K [24]. Subsequently, it was found that moderate annealing (around 500 K) helped to improve the perpendicular anisotropy in Ni/NiO multilayer films due to the partial recrystallization of initially amorphous NiO layers [25]. This led to an increase in the magnetoelastic anisotropy of the system, while the surface anisotropy remained almost the same [25].

Recently, studies on Co/CoO [26] and Ni$_{0.9}$Co$_{0.1}$/NiCoO [27] multilayers were carried out, wherein loops of inverted hysteresis, exchange bias, and PMA were predominantly observed at low temperatures. These characteristics render these systems interesting for investigations in antiferromagnetic spintronics. Moreover, multilayered films of Co/CoO/Pt were studied, revealing the optimal combination of properties, including large coercive fields, perpendicular anisotropy, and exchange bias [28]. NiO antiferromagnetic layers, either as an insertion in a stack or in trilayer form, have attracted the interest of many studies in ultrafast spintronics [29–31]. In a recent study, the role of a thin antiferromagnetic NiO layer was examined as an intermediate in a trilayer with Ni/NiO/Pt form, and it showed interesting results in transporting ultrafast spin currents [32]. Consequently, in the present work, we deal with a case study of a Ni/NiO multilayer with intercalating ultrathin Pt layers and report on temperature-dependent magnetic properties. Specifically, we explore a multilayered Ni/NiO film with t_{Ni} = 6.7 nm and the addition of ultrathin Pt interlayers, both before and after mild thermal annealing at 250 °C for 90 min. We report on the multilayer structure, investigated by X-ray reflectivity (XRR) measurements before and after thermal annealing. Finally, an extensive comparison of magnetic anisotropy values between the two multilayers was conducted.

2. Materials and Methods

The high vacuum chamber where the deposition of the films took place had a base pressure of 3×10^{-7} mbar. Thin Ni/NiO/Pt multilayers were grown on Si(001) and Corning glass wafers by two radio-frequency (RF, the Torus 2 HV circular sputtering source of Kurt J. Lesker Company, Jefferson Hills, PA, USA) magnetron sputtering heads. The deposition was carried out under argon pressure, $P_{Ar} = 3 \times 10^{-3}$ mbar, and RF power operating at 30 W for the Ni layers, and under argon pressure, $P_{Ar} = 1 \times 10^{-2}$ mbar, and 20 W for the Pt layers.

The thickness of each metallic layer was measured in situ using a pre-calibrated piezoelectric quartz balance system (Inficon XTM/2, Kurt J. Lesker Company, Jefferson Hills, PA, USA) with an accuracy of ± 0.1 nm. The thickness and layering quality of multilayers were confirmed through the X-ray reflectivity (XRR) technique, showing good agreement with the preset deposition time and desired thickness values. X-ray reflectivity measurements were performed using a Bruker D8 diffractometer (Bruker, D8-Advance, Karlsruhe, Germany) and focused Cu-K$_{\alpha 1}$ radiation ($\lambda = 0.15418$ nm). For the formation of the NiO layer, we performed natural oxidation. With this method, after the deposition of every Ni layer, a fine valve was opened to let air enter the chamber for approximately one minute at a partial pressure of around 2.5×10^{-3} mbar. The Ni/NiO bilayer was then formed, with the thickness of the saturated oxidized layer remaining constant at about $t_{NiO} = 1.4 \pm 0.2$ nm [24]. A 5 nm Pt layer was deposited first on each substrate and finally, on top of the sample to prevent oxidation after exposure to air serving as a buffer and capping layer, respectively. This procedure was repeated n = 5 times, resulting in the final composition of our multilayers: Pt/[Ni/NiO/Pt]n/Pt. The sample's total thickness was approximately 50 nm. We did not grow thicker multilayers since they generally exhibit a higher density of defects [33]. A multilayered film with a precise composition of Pt(5 nm)/[Ni(6.7 nm)/NiO(1.4 nm)/Pt(0.4 nm)]$_5$/Pt(5 nm) was selected for magnetic measurements. We have selected this value of t_{Ni} because the corresponding Ni/NiO multilayer with similar t_{Ni} showed the best tendency for PMA after annealing [25]. On the other hand, the choice of such thin Pt layers was based on the favorable development of perpendicular anisotropy observed in the Ni/Pt system [6,7]. Finally, a 5 nm Pt capping layer was deposited on top of the sample to prevent oxidation after exposure to air.

The magnetic properties of films were performed with a Quantum Design SQUID VSM magnetometer (Quantum Design, Darmstadt, Germany) in applied fields of up to 40 kOe in the temperature range of 4–300 K. The procedural protocol comprised an initial field-cooling stage, the establishment of the temperature parameter, followed by the execution of magnetic hysteresis loop cycles ranging from the positive maximum saturation field to the negative maximum field and returning to the positive maximum field. This approach ensures the elimination of any potential experimental errors that may impact the magnetization reversal.

3. Results

3.1. Multilayer Structural Characterization

Figure 1 illustrates the XRR pattern of our multilayer in the as-deposited state, Figure 1a, and after annealing in air at 250 °C for 90 min, Figure 1b. X-ray reflectivity oscillations are evident for both samples, revealing well-defined interfaces and homogeneous film thickness. Given the diverse individual layer thicknesses within each sample, distinguishing between the Bragg and Kiessig fringes [34] proves challenging, resulting in an overlap between them. Consequently, to extract quantitative details regarding the overall or specific layer thickness and the roughness of individual bilayers in our samples, we conducted fits of the XRR patterns utilizing the GenX 3 software package [35]. The thickness values obtained from the GenX fitting align closely with those presented in the preceding section. Furthermore, these values exhibit satisfactory agreement with the indications of our pre-calibrated quartz balance system for the determination of growth rates during deposition. The root-mean-square (RMS) roughness values for the Ni, Pt, and NiO layers consistently remain below 1 nm (RMS$_{Ni}$ = 0.3, RMS$_{Pt}$ = 0.2, and RMS$_{NiO}$ = 0.7 nm, respectively).

After annealing, we recorded again the XRR pattern of the sample. This pattern is modified compared to the one in Figure 1a. The RMS roughness of the layers shows an increase for all layers after annealing, approximately doubling. Specifically, the values become 0.8 nm for Ni, 0.4 nm for Pt, and 1.4 nm for NiO. Overall, it appears that the annealing process resulted in increased layer roughness for Ni/NiO/Pt multilayers and/or

some interdiffusion. This suggests that the periodicity has slightly degraded during the annealing procedure.
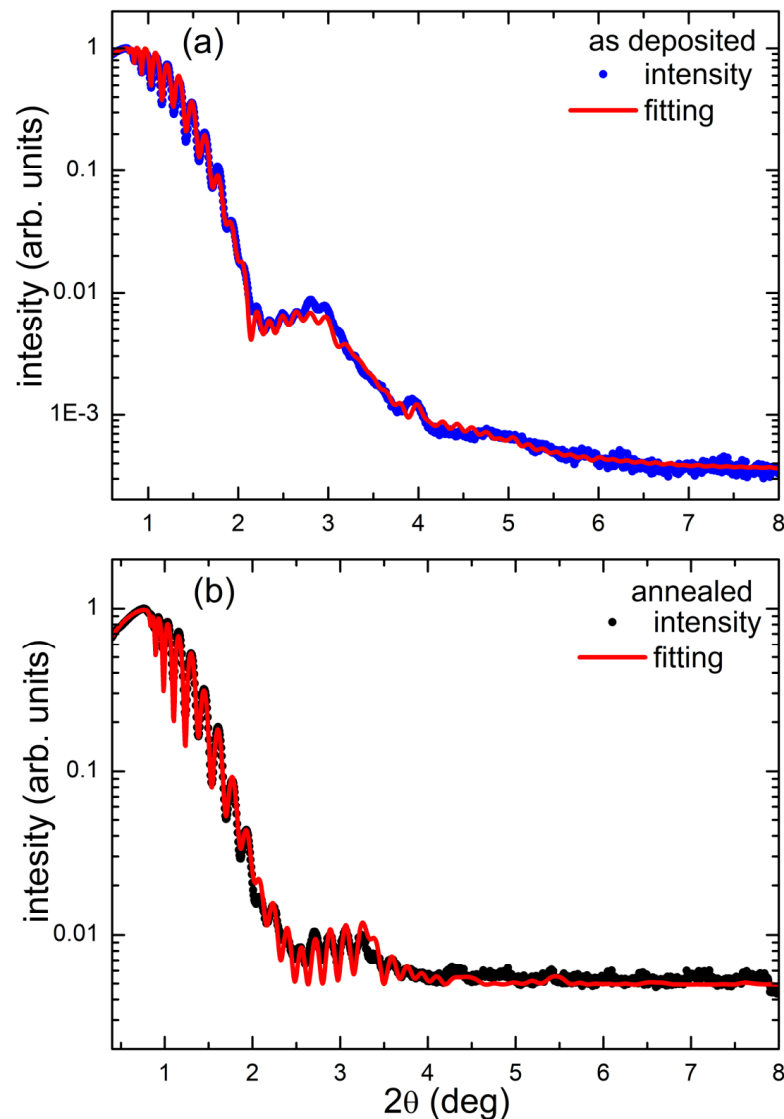
Figure 1. XRR patterns for a Ni/NiO/Pt multilayer (data points) in (**a**) the as-deposited state and (**b**) after annealing. The fitted patterns using the GenX code are also shown (continuous lines).

3.2. Multilayer Magnetic Characterization

Figure 2a presents the magnetization hysteresis loops under parallel and perpendicularly applied magnetic fields at 300 K for the sample before annealing. In Figure 2b, the hysteresis loops for 10 K are shown. The saturation magnetization M_S is approximately M_S = 426.6 emu/cm^3-Ni. At 10 K, bulk Ni should possess a magnetization of M_{Ni} = 510 emu/cm^3 [36]. The decrease in the saturation magnetization value of our sample may be due to partial interdiffusion of Pt and Ni at the interface, which affects the magnetization value [7–9]. Moreover, there is always an additional error of the order of 5–10%, mainly due to uncertainty in calculating the volume of magnetic layers. Overall, this sample saturates easier in the film plane; thus, it shows in-plane anisotropy, and the loops with the field applied along the film normal are typical hard-axis loops (Figure 2a). At lower temperatures, the behavior slightly changes. At 10 K, the saturation of the longitudinal loop is reached more gradually (Figure 2b). Moreover, both hysteresis loops show an

increase in coercive field (Hc) and saturation magnetization in both applied fields parallel and perpendicular to the film plane.
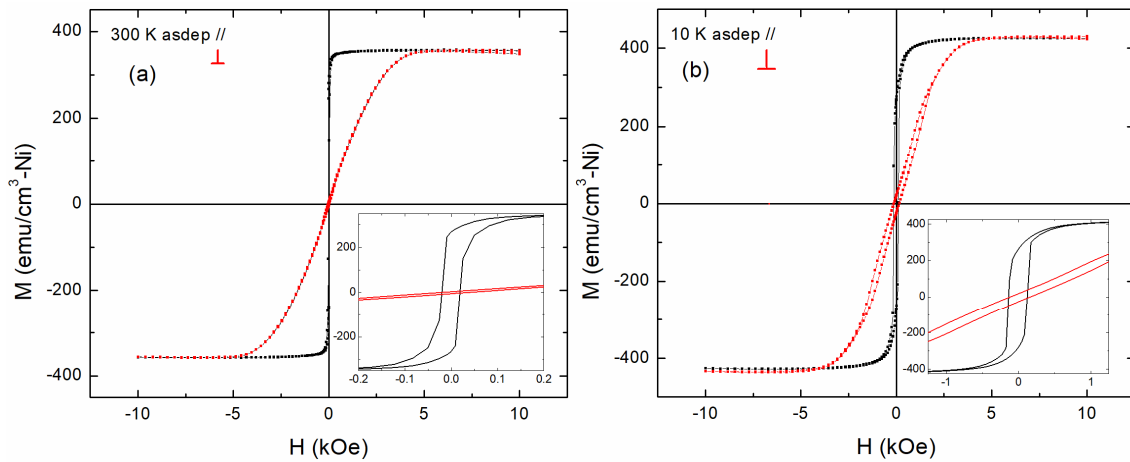

Figure 2. In-plane and out-of-plane hysteresis curves of Ni/NiO/Pt multilayers in the as-deposited state with SQUID magnetometry. Curves were measured (**a**) at T = 300 K and (**b**) at T = 10 K. The insets are zoom-ins for better visibility.

In Figure 3a, we present the temperature-dependent saturation magnetization Ms(T). One may assume that the Curie point of our multilayer with relatively thick nickel layers should not be much smaller than that of bulk Nickel (approximately 627 K [36]). Moreover, it is well known that up to about 30% of T_C is in the spin-wave regime [36]. Then, one may fit the temperature dependence of magnetization up to 200 K using the classical Bloch's law [36]:

$$M(T) = M_S(0) \times [1 - A \times T^{3/2}] \tag{1}$$

where A is a constant that, for bulk Ni, has a value of $0.75 \times 10^{-5} \text{ deg}^{-3/2}$. The fitting in Figure 3b gives for our film the value $A = 2.5 \times 10^{-5} \text{ deg}^{-3/2}$, which is larger than the one of bulk nickel and even slightly larger than the one for the multilayer $6 \times \text{Ni}(7 \text{ nm})/\text{NiO}$ (1.4 nm) in Ref. [24]. Multilayers' temperature-dependent magnetizations always show a larger value of A than bulk materials due to finite-size effects [37].
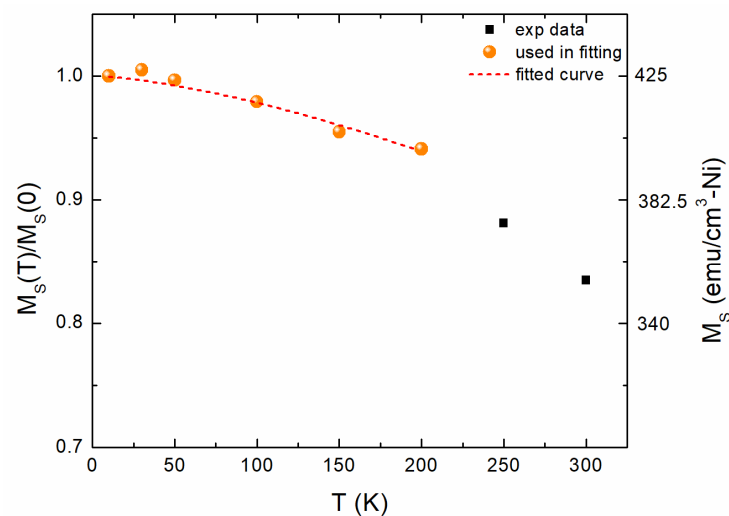
Figure 3. Temperature dependence of saturation magnetization M_S (right Y axis) and its normalized value [$M_S(T)/M_S(0)$] (left Y axis), for the multilayer in the as-deposited state between 10–300 K. The fitting process is based on Equation (1) and is depicted with a red dashed line.

Figure 4 presents temperature-dependent remanence magnetization, M_R, and the coercive field, H_C, for the as-deposited sample. As we have seen in Figure 2, the remanent magnetization for the parallel field increases at room temperature. This is related to the commonly observed effect of a uniaxial anisotropy, which decreases faster than the shape anisotropy, as we will discuss below.
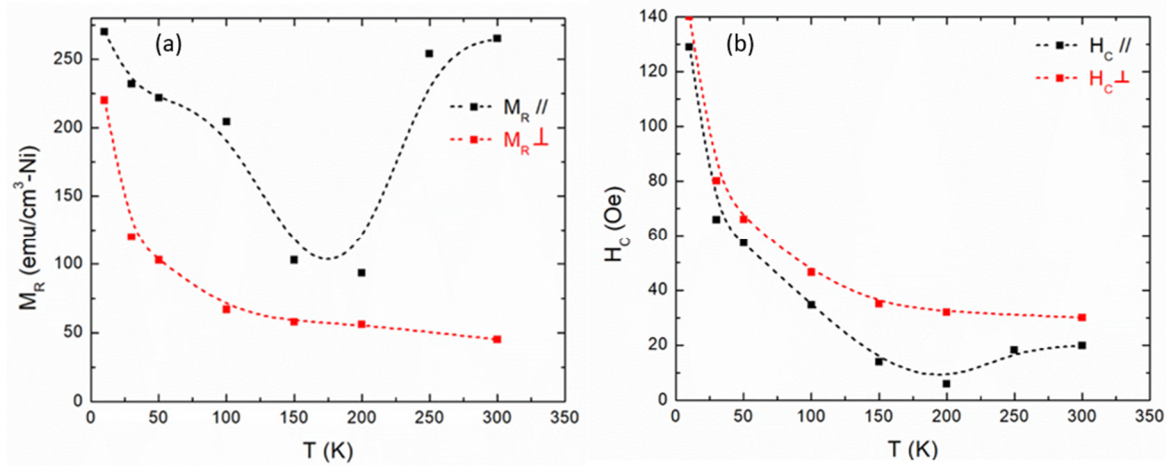
Figure 4. (**a**) Temperature dependence of remanent magnetization, M_R, in parallel and perpendicular external fields for the Ni/NiO/Pt film before annealing. (The lines are provided as guides to the eye.) (**b**) Temperature dependence of the coercive field, H_C, in parallel and perpendicular external fields for the Ni/NiO/Pt film before annealing.

The so-called effective anisotropy constant, K_{eff}, is defined as the area between the easy- and hard-magnetization axes Figure 4 presents temperature-dependent remanence magnetization, M_R, and the coercive field, H_C for the as-deposited sample. As we have seen in Figure 2, the remanent magnetization for the parallel field increases at room temperature. This is related to the commonly observed effect of a uniaxial anisotropy which decreases faster than the shape anisotropy, as we will discuss below.

The so-called effective anisotropy constant, K_{eff}, is defined as the area between the easy- and hard- magnetization axis [38]. This can be defined by the relationship:

$$K_{eff} = K_u - 2\pi M s^2 \qquad (2)$$

where the term $2\pi M s^2$ is the shape anisotropy of a thin film, and K_u is the first-order uniaxial anisotropy constant, which is the dominant one in polycrystalline films due to the cylindrical symmetry of the system (isotropic in the film plane). K_u includes all contributions (magnetocrystalline, magnetoelastic, interfacial, and surface anisotropy), and when it is positive, then it favors the perpendicular to the film plane direction to be an easy magnetization axis. This property (PMA) is desirable for technological applications [39]. However, as shape anisotropy competes against uniaxial anisotropy, for the actual existence of an out-of-plane easy magnetization axis, K_{eff} should be positive too. Figure 5 presents the evolution of the various anisotropy contributions as a function of temperature.

An interesting observation is that the shape anisotropy and uniaxial anisotropy vary almost in parallel, resulting in nearly constant effective anisotropy. In fact, it even slightly increases with temperature towards room temperature, leading to an increase in M_R and H_C in the parallel field near room temperature, as Figure 4 reveals. On the other hand, the theory predicts the temperature dependence of shape anisotropy from the square of the normalized magnetization $M_{red} = M_S(T)/M_S(0)$ and that of the normalized uniaxial anisotropy from the cube of the normalized magnetization, indicating a faster decrease with temperature [40,41]. In Figure 6, we compare the temperature variations of the normalized

uniaxial anisotropy in order to verify if the normalized uniaxial anisotropy follows the third power of normalized magnetization. The attempted fitting is based on the following:

$$K_u(T)/K_u(10) = [M_{red}]^\Gamma \tag{3}$$
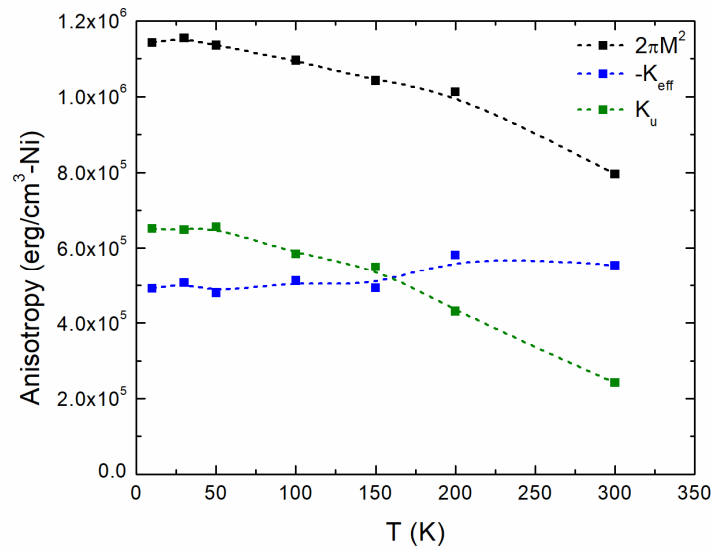
Figure 5. Temperature dependence of anisotropy contributions for Ni/NiO/Pt sample before annealing. (The lines are provided as guides for better visualization.)
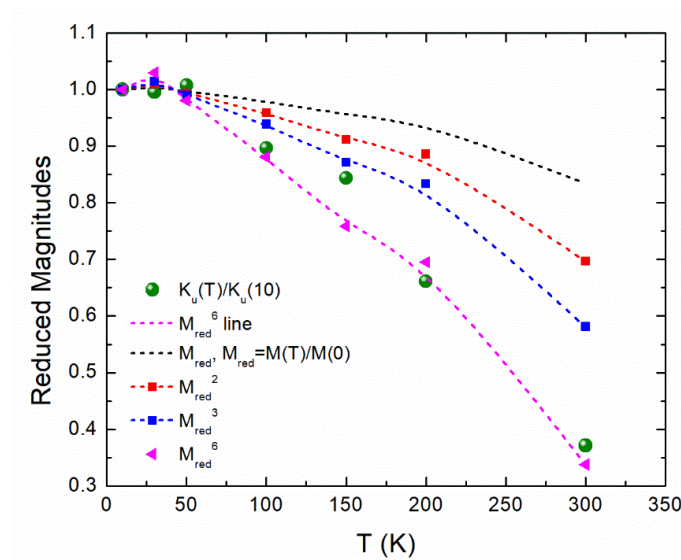

Figure 6. Temperature dependence of uniaxial anisotropies for Ni/NiO/Pt film before annealing. The experimental data are compared to powers of reduced magnetization. The experimental data seem to follow a decrease close to the sixth power of reduced magnetization.

Instead of finding dependence on the third power of normalized magnetization, we find dependence on the sixth power. This is interesting because the same temperature dependence was observed in a similar sample in reference [24], while other samples with thinner Ni layers showed dependence on a smaller power. This was attributed to the contribution of higher-order uniaxial anisotropy terms [24].

In Figure 7, we show SQUID magnetometry measurements carried out at 300 K (Figure 7a), and 10 K (Figure 7b) for the multilayer after annealing. This investigation aligns well with the results of Ref. [25]. The annealing conditions in the present work are

the same as those used for the samples discussed in reference [25]. In Ref. [25], the XRR and high-resolution transmission electron microscopy (HRTEM) experiments demonstrated a marginal increase in roughness even for thinner Ni layers compared to the 6.7 nm utilized in the present study. The satisfactory degree of layering of Ni and NiO was maintained after annealing.
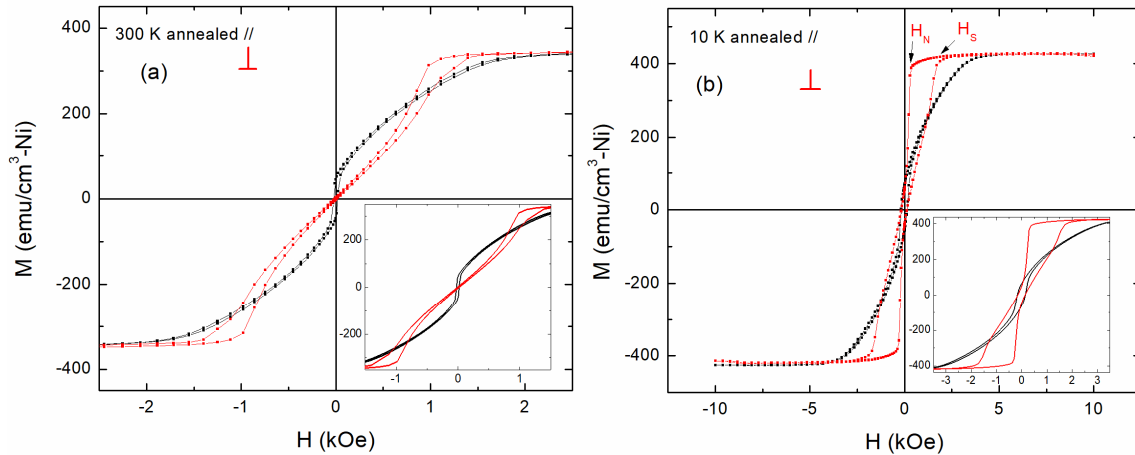

Figure 7. In-plane and out-of-plane hysteresis curves of Ni/NiO/Pt multilayers after mild thermal annealing at 250 °C for 90 min, were obtained with SQUID magnetometry. Curves were measured (**a**) at T = 300 K and (**b**) at T = 10 K. The insets are zoom-ins for better visibility.

For the loops with the field applied perpendicular to the field plane, one may observe a drastic change compared to the ones in Figure 2: one may identify a H_N (nucleation field), where it is known that perpendicular magnetic bubble domains appear. This is concluded by the characteristic shape of the loop; for example, see Ref. [42]. Kashuba and Pokrovsky found that the mathematical expression of the magnetization as a function of the field below H_N for an ideal curve without hysteresis for films breaking into domains is of the form $M \propto \arcsin(H/H_N)$ [43,44]. This phenomenon is clearer at T = 10 K, where the perpendicular direction clearly becomes an easy axis, as is shown in Figure 7b. On the other hand, at room temperature, the loops with the field applied parallel or perpendicular to the film plane are twisted one to the other, and the only way to get an idea of which axis is easy is to find the sign of the area between them. The significant decrease in the saturation field H_S in the perpendicular field direction as temperature decreases may indicate that a spin reorientation transition (SRT) takes place. We will come back to this in Section 4.

A comparison of the hysteresis loops in Figures 2 and 7 reveals a striking increase in PMA after annealing. This observation aligns with the findings of Ref. [25], where a similar phenomenon was observed after annealing. It was attributed to the partial recrystallization of the initially amorphous NiO layers with post-annealing [25]. This transformation is accompanied by an increase in residual stresses at the Ni/NiO interface, which amplifies the magnetoelastic anisotropy and, consequently, promotes perpendicular magnetic anisotropy [25].

Figure 8 illustrates the temperature dependence of magnetization M_S before and after annealing, between 10 and 300 K. We observe a tiny decrease in magnetization in the annealed sample. This could be attributed to some further interdiffusion occurring at the Ni and Pt interface, leading to a slight reduction in the T_C. Consequently, the magnetization in the annealed sample exhibits a slightly faster decrease with temperature compared to the as-deposited one.
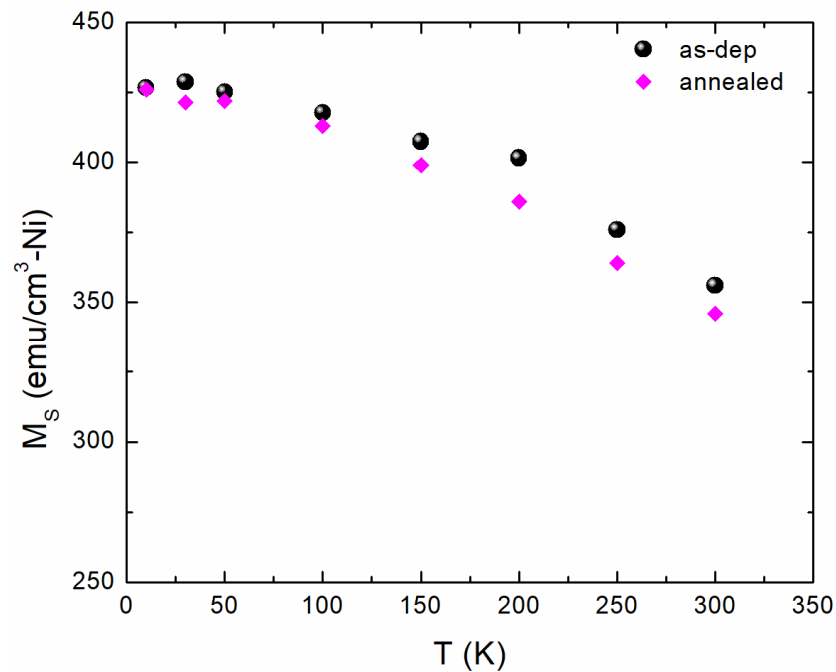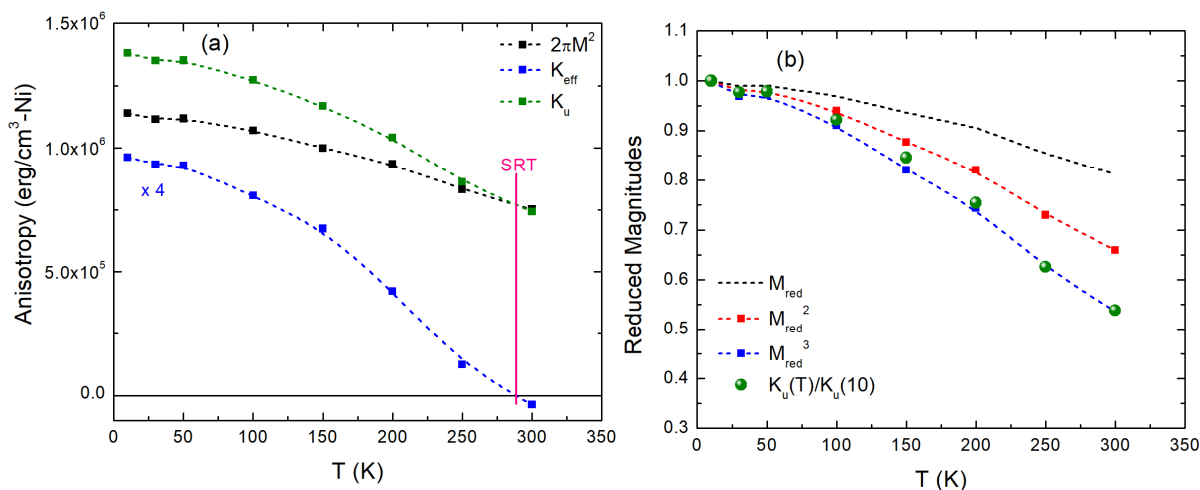
Figure 8. Temperature dependence of saturation magnetization M_S for the Ni/NiO/Pt multilayer before and after annealing.

To find the anisotropy when loops exhibit moderate hysteresis, we used the averaging of the two branches with the field ascending and descending, as shown, for example, in Figure 9. This removes hysteresis, and it is useful in the evaluation of the anisotropies by the area between the parallel and perpendicular fields when hysteresis is considerable. In Figure 10a, we show the temperature-dependent anisotropy contributions of the film after annealing. The uniaxial anisotropy curve crosses the shape anisotropy just below room temperature. As a result, K_{eff} changes signs. This, in the single-domain or Stoner-Wolfarth approximation, may be traditionally interpreted as a change of the easy-axis direction or, equivalently, as an SRT; see, e.g., [45] and references therein. In Figure 10b, the reduced anisotropy after annealing seems to follow the cube of the temperature dependence of the reduced magnetization, satisfying the Callen and Callen predictions [40].
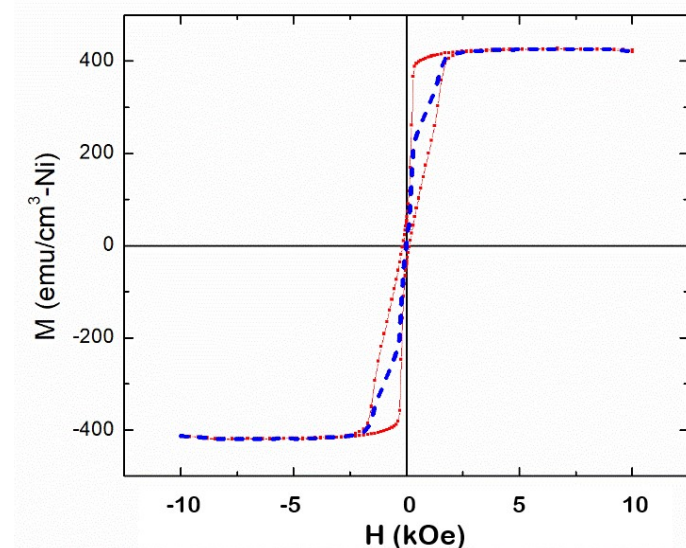
Figure 9. Hysteresis loop and averaging curve (with zero hysteresis) for the annealed Ni/NiO/Pt film at 10 K (perpendicular field direction).

Figure 10. (**a**) Temperature dependence of the anisotropy values for the Ni/NiO/Pt film after annealing. The lines are provided as guides for better visualization. Notably, at 289 K, there is a change of sign in K_{eff}. Additionally, (**b**) the temperature dependence of uniaxial anisotropies for the Ni/NiO/Pt film after annealing are depicted in.

4. Discussion

First, we discuss the effect of Pt interlayers on the magnetic properties of the Ni/NiO multilayers. In Ref. [25], we showed enhanced PMA in Ni/NiO multilayers after annealing; however, magnetic remanence was small due to the formation of magnetic domains with spins up or down with respect to the film plane. In this work, we fabricated Ni/NiO/Pt multilayers with the aim of reducing the values of the nucleation field H_N or even increasing the remanence. Platinum is an easily spin-polarizable element. Therefore, it may acquire a considerable induced magnetic moment upon alloying with ferromagnetic elements and at the interfaces with magnetic layers such as Ni; see, e.g., Ref. [8]. Direct orbital hybridization between Pt and Ni produces a spin polarization of Pt, while the large spin-orbit coupling of the heavy element 5*d* Pt is transmitted to Ni, resulting in enhanced magneto-optical properties and magnetic anisotropies [45], which in our case favor PMA. Moreover, the limited deterioration of layered quality after annealing observed by XRR may suggest the formation of some NiPt alloy at the interface. This, in turn, may possess residual strain, further enhancing the magnetoelastic anisotropy. We have to state here that there are also other interesting systems, such as iron-substituted strontium titanate single-layer films, with the oxygen concentration and partial pressure during growth playing an important role in the magnetic and magneto-optical properties, but their nature is quite different from our multilayers [46].

The effect of Pt in the enhancement of PMA is evident if one compares the value of the nucleation field at R.T. in our sample with the one in [25] after annealing for the film with the same individual Ni layer thickness. In Ref. [25], H_N = 1.5 kOe, while the corresponding value for the film with a Pt interlayer in the current work is only 1 kOe. Since nothing else changed between the two films or the annealing process, the decrease in H_N is due to Pt. This shows enhanced PMA in Ni/NiO/Pt compared to Ni/NiO multilayers.

Second, we turn to a brief discussion on spin reorientation and magnetic domains. When one evaluates magnetic properties at magnetic saturation, like, e.g., saturation magnetization, the use of a single-domain (Stoner-Wolfarth [47]) model is appropriate. Techniques such as Ferromagnetic Resonance and Torque Magnetometry are very accurate in the determination of magnetic anisotropy constants too, as they perform measurements under external fields that are large enough to annihilate domains. In the classical model, of a single domain, magnetization reversal takes place via rotation. Within this model at a specific temperature of about 289 K, K_{eff} changes sign, and accordingly, following Equation (2), the easy-magnetization axis should have changed from perpendicular to the

film plane to parallel. However, the appearance of magnetic domains near remanence complicates the evaluation of magnetic anisotropies from static measurements, like, e.g., hysteresis loops. Our multilayer after annealing shows at all temperatures sheared loops recorded with the field applied perpendicularly to the film plane. These loops are indicative of the presence of magnetic domains when the field is smaller than the nucleation field [42, 48]. This field is very small at low temperatures and increases with temperature. Following Refs. [44,49], as temperature increases, one may expect a change of spin state from up and down magnetic domains to in-plane magnetization only at a transition temperature T_r when the remanence of the hysteresis loop recorded with the field applied parallel to the film plane exceeds a value of 50% [44]. The very small values of remanent magnetization with the field applied parallel to the film plane even at T = 300 K, on the other hand, show that when the parallel magnetic field decreases from saturation to zero, the magnetization is redirected from the in-plane to a spin up and down domain state with possible canting [42, 50]. Therefore, the exact temperature where the SRT takes place depends on the model one adopts. In the presence of magnetic domains, the concept of a clear SRT may be oversimplified.

Finally, the comparison of the results between Figures 6 and 10b may suggest a significant and potentially, to our knowledge, new observation. The temperature dependence of the uniaxial anisotropy, before annealing, follows the 6th power of the change of the reduced magnetization, like the corresponding multilayer film in Ref. [24]. After annealing, however, the same magnitude follows the 3rd power of reduced magnetization, precisely as predicted by the thermodynamic model of Callen and Callen for first-order uniaxial anisotropy [40]. The simplest assertion we can make is that, since the uniaxial anisotropy doubled after annealing (Figures 5 and 10a at 10 K), its role compared to the second-order anisotropy was reinforced. Furthermore, we believe that the structural changes observed in Ref. [25] not only doubled the value of the first-order uniaxial anisotropy but also diminished the value of the second-order anisotropy due to the better crystallization of NiO layers [25]. Further exploration of this intriguing topic extends beyond the scope of this work.

5. Conclusions

In this work, we investigate the magnetic properties of Ni/NiO/Pt multilayers before and after annealing at 250 °C in a furnace with air. The samples were deposited using an RF magnetron sputtering technique, demonstrating very good layer quality with small roughness values, as revealed by XRR measurements. SQUID magnetometry was employed to study temperature-dependent magnetizations and anisotropy values. In the as-deposited state, easy-plane behavior is observed in the samples, typical of polycrystalline magnetic thin films. After annealing, perpendicular magnetic anisotropy becomes predominant in the system. In conclusion, we demonstrated the significant role of ultrathin Pt layers in the system regarding PMA enhancement compared to the Ni/NiO ones. The Ni/NiO/Pt multilayers can be potentially useful for applications related to spintronics and magnetic storage.

Author Contributions: Conceptualization, P.P. and D.I.A.; methodology, P.P., D.I.A., C.M.T. and E.T.P.; software, C.M.T., P.P. and D.I.A.; validation, P.P., E.T.P. and G.S.; formal analysis, D.I.A., A.B. and N.C.D.; investigation, D.I.A., C.M.T., A.B. and N.C.D.; resources, P.P., E.T.P. and G.S.; data curation, D.I.A. and A.B.; writing—original draft preparation, D.I.A.; writing—review and editing, P.P., E.T.P., C.M.T., N.C.D. and G.S.; visualization, P.P., E.T.P. and G.S.; supervision, P.P. and E.T.P.; project administration, P.P. All authors have read and agreed to the published version of the manuscript.

Data Availability Statement: Data is contained within the article.

Conflicts of Interest: The authors declare no conflicts of interests.

References

1. Carcia, P.F.; Meinhaldt, A.D.; Suna, A. Perpendicular magnetic anisotropy in Pd/Co thin film layered structures. *Appl. Phys. Lett.* **1985**, *47*, 178–180. [CrossRef]
2. Hashimoto, S.; Ochiai, Y. Co/Pt and Co/Pd multilayers as magneto-optical recording material. *J. Magn. Magn. Mater.* **1990**, *88*, 211–226. [CrossRef]
3. Chappert, C.; Fert, A.; Van Dau, F.N. The emergence of spin electronics in data storage. *Nat. Mater.* **2007**, *6*, 813–823. [CrossRef] [PubMed]
4. Hirohata, A.; Yamada, K.; Nakatani, Y.; Prejbeanu, I.-L.; Dieny, B.; Pirro, P.; Hillebrands, B. Review on spintronics: Principles and device applications. *J. Magn. Magn. Mater.* **2020**, *509*, 166711. [CrossRef]
5. Krishnan, R.; Lassri, H.; Porte, M.; Tessier, M.; Renaudin, P. Perpendicular magnetization in Ni/Pt multilayers. *Appl. Phys. Lett.* **1991**, *59*, 3649–3650. [CrossRef]
6. Angelakeris, M.; Poulopoulos, P.; Vouroutzis, N.; Nyvlt, M.; Prosser, V.; Visnovsky, S.; Krishnan, R.; Flevaris, N.K. Structural and spectroscopic magneto-optic studies of Pt-Ni multilayers. *J. Appl. Phys.* **1997**, *82*, 5640–5645. [CrossRef]
7. Shin, S.-C.; Srinivas, G.; Kim, Y.-S.; Kim, M.-G. Observation of perpendicular magnetic anisotropy in Ni/Pt multilayers at room temperature. *Appl. Phys. Lett.* **1998**, *73*, 393. [CrossRef]
8. Wilhelm, F.; Poulopoulos, P.; Ceballos, G.; Wende, H.; Baberschke, K.; Srivastava, P.; Benea, D.; Ebert, H.; Angelakeris, M.; Flevaris, N.K.; et al. Layer-Resolved Magnetic Moments in Ni/Pt Multilayers. *Phys. Rev. Lett.* **2000**, *85*, 413. [CrossRef]
9. Kim, Y.-S.; Shin, S.-C. Origin of room-temperature perpendicular magnetic anisotropy in Ni/Pt multilayers. *Phys. Rev. B* **1999**, *59*, R6597. [CrossRef]
10. Ohring, M. *Materials Science of Thin Films*, 2nd ed.; Academic Press: San Diego, CA, USA, 2002.
11. Krishnan, R.; Lassri, H.; Prasad, S.; Porte, M.; Tessier, M. Magnetic properties of Ni/Pt multilayers. *J. Appl. Phys.* **1993**, *73*, 6433. [CrossRef]
12. Moodera, J.S.; Kinder, L.R.; Wong, T.M.; Meservey, R. Large Magnetoresistance at Room Temperature in Ferromagnetic Thin Film Tunnel Junctions. *Phys. Rev. Lett.* **1995**, *74*, 3273. [CrossRef]
13. Nistor, L.E.; Rodmacq, B.; Auffret, S.; Dieny, B. Pt/Co/oxide and oxide/Co/Pt electrodes for perpendicular magnetic tunnel junctions. *Appl. Phys. Lett.* **2009**, *94*, 012512. [CrossRef]
14. Bibes, M.; Villegas, J.E.; Barthélémy, A. Ultrathin oxide films and interfaces for electronics and spintronics. *Adv. Phys.* **2011**, *60*, 5–84. [CrossRef]
15. Dieny, B.; Chshiev, M. Perpendicular magnetic anisotropy at transition metal/oxide interfaces and applications. *Rev. Mod. Phys.* **2017**, *89*, 025008. [CrossRef]
16. Baltz, V.; Manchon, A.; Tsoi, M.; Moriyama, T.; Ono, T.; Tserkovnyak, Y. Antiferromagnetic spintronics. *Rev. Mod. Phys.* **2018**, *90*, 015005. [CrossRef]
17. Blachowicz, T.; Ehrmann, A. Exchange bias in thin films—An update. *Coatings* **2021**, *11*, 122. [CrossRef]
18. Tsoi, M. Antiferromagnetic spintronics: From metals to functional oxides. *Low Temp. Phys.* **2023**, *49*, 786. [CrossRef]
19. May, F.; Tischer, M.; Arvanitis, D.; Russo, M.; Hunter Dunn, J.; Henneken, H.; Wende, H.; Chauvistré, R.; Mårtensson, N.; Baberschke, K. Modifications of the electronic and magnetic properties of ultrathin Ni/Cu(100) films induced by stepwise oxidation. *Phys. Rev. B* **1996**, *53*, 1076. [CrossRef]
20. Beach, G.S.D.; Berkowitz, A.E.; Parker, F.T.; Smith, D.J. Magnetically soft, high-moment, high-resistivity thin films using discontinuous metal/native oxide multilayers. *Appl. Phys. Lett.* **2001**, *79*, 224–226. [CrossRef]
21. Butler, W.H.; Zhang, X.G.; Schulthess, T.C.; MacLaren, J.M. Spin-dependent tunneling conductance of Fe|MgO|Fe sandwiches. *Phys. Rev. B* **2001**, *63*, 054416. [CrossRef]
22. Mulders, A.M.; Loosvelt, H.; Fraile Rodriguez, A.; Popova, E.; Konishi, T.; Temst, K.; Karis, O.; Arvanitis, D.; Van Haesendonck, C. On the interface magnetism of thin oxidized Co films: Orbital and spin moments. *J. Phys. Condens. Matter* **2009**, *21*, 124211. [CrossRef] [PubMed]
23. Yang, H.X.; Chshiev, M.; Dieny, B.; Lee, J.H.; Manchon, A.; Shin, K.H. First-principles investigation of the very large perpendicular magnetic anisotropy at Fe|MgO and Co|MgO interfaces. *Phys. Rev. B* **2011**, *84*, 054401. [CrossRef]
24. Pappas, S.D.; Kapaklis, V.; Delimitis, A.; Jönsson, P.E.; Papaioannou, E.T.; Poulopoulos, P.; Fumagalli, P.; Trachylis, D.; Velgakis, M.J.; Politis, C. Layering and temperature-dependent magnetization and anisotropy of naturally produced Ni/NiO multilayers. *J. Appl. Phys.* **2012**, *112*, 053918. [CrossRef]
25. Anyfantis, D.I.; Sarigiannidou, E.; Rapenne, L.; Stamatelatos, A.; Ntemogiannis, D.; Kapaklis, V.; Poulopoulos, P. Unexpected development of perpendicular magnetic anisotropy in Ni/NiO multilayers after mild thermal annealing. *IEEE Magn. Lett.* **2019**, *10*, 1–5.
26. Anyfantis, D.I.; Kanistras, N.; Barnasas, A.; Poulopoulos, P.; Papaioannou, E.T.; Conca, A.; Trachylis, D.; Politis, C. Effects of thermal annealing and Ni addition on the magnetic properties of Co–CoO multilayers. *SPIN* **2020**, *40*, 2050030. [CrossRef]
27. Anyfantis, D.I.; Kanistras, N.; Ballani, C.; Barnasas, A.; Kapaklis, V.; Schmidt, G.; Papaioannou, E.T.; Poulopoulos, P. Magnetic aspects and large exchange bias of $Ni_{0.9}Co_{0.1}$/NiCoO multilayers. *Micro* **2021**, *1*, 43–54. [CrossRef]
28. Anyfantis, D.I.; Ballani, C.; Kanistras, N.; Barnasas, A.; Tsiaoussis, I.; Schmidt, G.; Papaioannou, E.T.; Poulopoulos, P. Magnetic Anisotropies and Exchange Bias of Co/CoO Multilayers with Intermediate Ultrathin Pt Layers. *Materials* **2023**, *16*, 1378. [CrossRef]

29. Hahn, C.; De Loubens, G.; Naletov, V.V.; Ben Youssef, J.; Klein, O.; Viret, M. Conduction of spin currents through insulating antiferromagnetic oxides. *Europhys. Lett.* **2014**, *108*, 57005. [CrossRef]
30. Wang, H.; Du, C.; Hammel, P.C.; Yang, F. Antiferromagnonic spin transport from $Y_3Fe_5O_{12}$ into NiO. *Phys. Rev. Lett.* **2014**, *113*, 097202. [CrossRef]
31. Lin, W.; Chen, K.; Zhang, S.; Chien, C.L. Enhancement of thermally injected spin current through an antiferromagnetic insulator. *Phys. Rev. Lett.* **2016**, *116*, 186601. [CrossRef]
32. Kanistras, N.; Scheuer, L.; Anyfantis, D.; Barnasas, A.; Torosyan, G.; Beigang, R.; Crisan, O.; Poulopoulos, P.; Papaioannou, E.T. Magnetic Properties and THz Emission from Co/CoO/Pt and Ni/NiO/Pt Trilayers. *Nanomaterials* **2024**, *14*, 215. [CrossRef] [PubMed]
33. Heinrich, B.; Bland, J.A.C. *Ultrathin Magnetic Structures I*, 1st ed.; Springer: Berlin/Heidelberg, Germany, 1994; pp. 1–6.
34. Kiessig, H. Untersuchungen zur totalreflexion von röntgenstrahlen. *Ann. Phys.* **1931**, *402*, 715–768. [CrossRef]
35. Björck, M.; Andersson, G. GenX: An extensible X-ray reflectivity refinement program utilizing differential evolution. *J. Appl. Crystallogr.* **2007**, *40*, 1174–1178. [CrossRef]
36. Kittel, C. *Introduction to Solid State Physics*, 5th ed.; John Wiley & Sons: New York, NY, USA, 1976.
37. Bergholz, R.; Gradmann, U. Structure and magnetism of oligatomic Ni(111)-films on Re(0001). *J. Magn. Magn. Mater.* **1994**, *45*, 389. [CrossRef]
38. Den Broeder, F.J.A.; Hoving, W.; Bloemen, P.J.H. Magnetic anisotropy of multilayers. *J. Magn. Magn. Mater.* **1991**, *93*, 562–570. [CrossRef]
39. De Jonge, W.J.M.; Bloemen, P.J.H.; den Broeder, F.J.A. Experimental investigations of magnetic anisotropy. In *Ultrathin Magnetic Structures I*, 2nd ed.; Springer: Berlin, Germany, 1994; pp. 65–90.
40. Callen, H.B.; Callen, E. The present status of the temperature dependence of magnetocrystalline anisotropy, and the l(l+1)/2 power law. *J. Phys. Chem. Solids* **1966**, *27*, 1271.
41. Zakeri, K.; Kebe, T.; Lindner, J.; Farle, M. Power-law behavior of the temperature dependence of magnetic anisotropy of uncapped ultrathin Fe Films on GaAs(001). *Phys. Rev. B* **2006**, *73*, 052405. [CrossRef]
42. Hehn, M.; Padovani, S.; Ounadjela, K.; Bucher, J.P. Nanoscale magnetic domain structures in epitaxial cobalt films. *Phys. Rev. B* **1996**, *54*, 3428. [CrossRef]
43. Kashuba, A.B.; Pokrovsky, V.L. Stripe domain structures in a thin ferromagnetic film. *Phys. Rev. B* **1993**, *48*, 10335. [CrossRef]
44. Berger, A.; Hopster, H. Magnetization reversal properties near the reorientation phase transition of ultrathin Fe/Ag(100) films. *J. Appl. Phys.* **1996**, *79*, 5619. [CrossRef]
45. Guo, G.Y.; Ebert, H. On the origins of the enhanced magneto-optical Kerr effect in ultrathin Fe and Co multilayers. *J. Magn. Magn. Mater.* **1996**, *156*, 173. [CrossRef]
46. Goto, T.; Kim, D.H.; Sun, X.; Onbasli, M.C.; Florez, J.M.; Ong, S.P.; Vargas, P.; Ackland, K.; Stamenov, P.; Aimon, N.M.; et al. Magnetism and Faraday Rotation in Oxygen-Deficient Polycrystalline and Single-Crystal Iron-Substituted Strontium Titanate. *Phys. Rev. Appl.* **2017**, *7*, 024006. [CrossRef]
47. Jiles, D. *Introduction to Magnetism and Magnetic Materials*, 1st ed.; Chapman and Hall: New Delhi, India, 2015.
48. Algaidi, H.; Zhang, C.; Ma, Y.; Liu, C.; Chen, A.; Zheng, D.; Zhang, X. Fe_3GaTe_2 with above-room-temperature ferromagnetism. *APL Mater.* **2024**, *12*, 011124. [CrossRef]
49. Allenspach, R.; Bischof, A. Magnetization direction switching in Fe/Cu(100) epitaxial films: Temperature and thickness dependence. *Phys. Rev. Lett.* **1992**, *69*, 3385. [CrossRef]
50. Frömter, R.; Stillrich, H.; Menk, C.; Oepen, H.P. Imaging the cone state of the spin reorientation transition. *Phys. Rev. Lett.* **2008**, *100*, 207202. [CrossRef]